



## Supporting Information

for *Adv. Sci.*, DOI: 10.1002/advs. 201500176

A Biomineralization Strategy for “Net”-Like Interconnected  
TiO<sub>2</sub> Nanoparticles Conformably Covering Reduced Graphene  
Oxide with Reversible Interfacial Lithium Storage

*Qiang Zhang, Yong Yan, and Ge Chen\**

## Supporting Information

### Title

Bio-mineralization Strategy toward “Net”-like Interconnected TiO<sub>2</sub> Nanoparticles  
Conformably Covering Reduced Graphene Oxide with Reversible Interfacial Lithium Storage

*Qiang Zhang, Yong Yan<sup>‡</sup> and Ge Chen\**

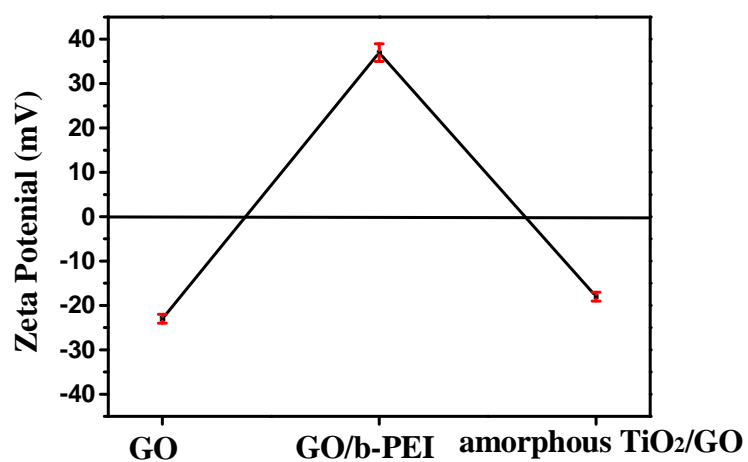


**Figure S1.** Zeta potentials of GO, GO/b-PEI, and amorphous TiO<sub>2</sub>/GO composites.

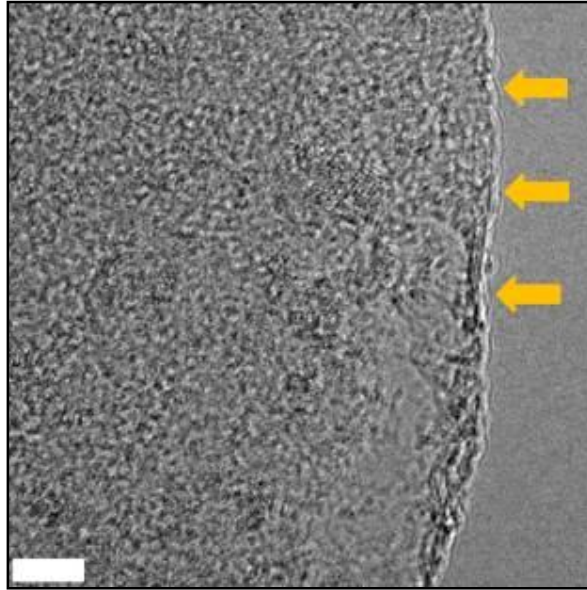


**Figure S2.** HRTEM image of amorphous TiO<sub>2</sub>/GO composite; the edge of GO marked by the orange arrow indicates the ultrathin nature (3–4 layers), bar 5 nm.

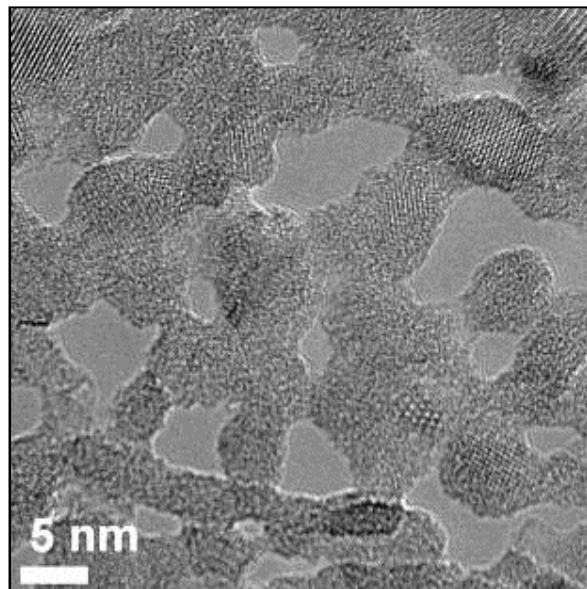


**Figure S3.** HRTEM image of anatase TiO<sub>2</sub>/RGO composite, indicating the “net”-like structure of TiO<sub>2</sub> conformably covering RGO, bar 5 nm.

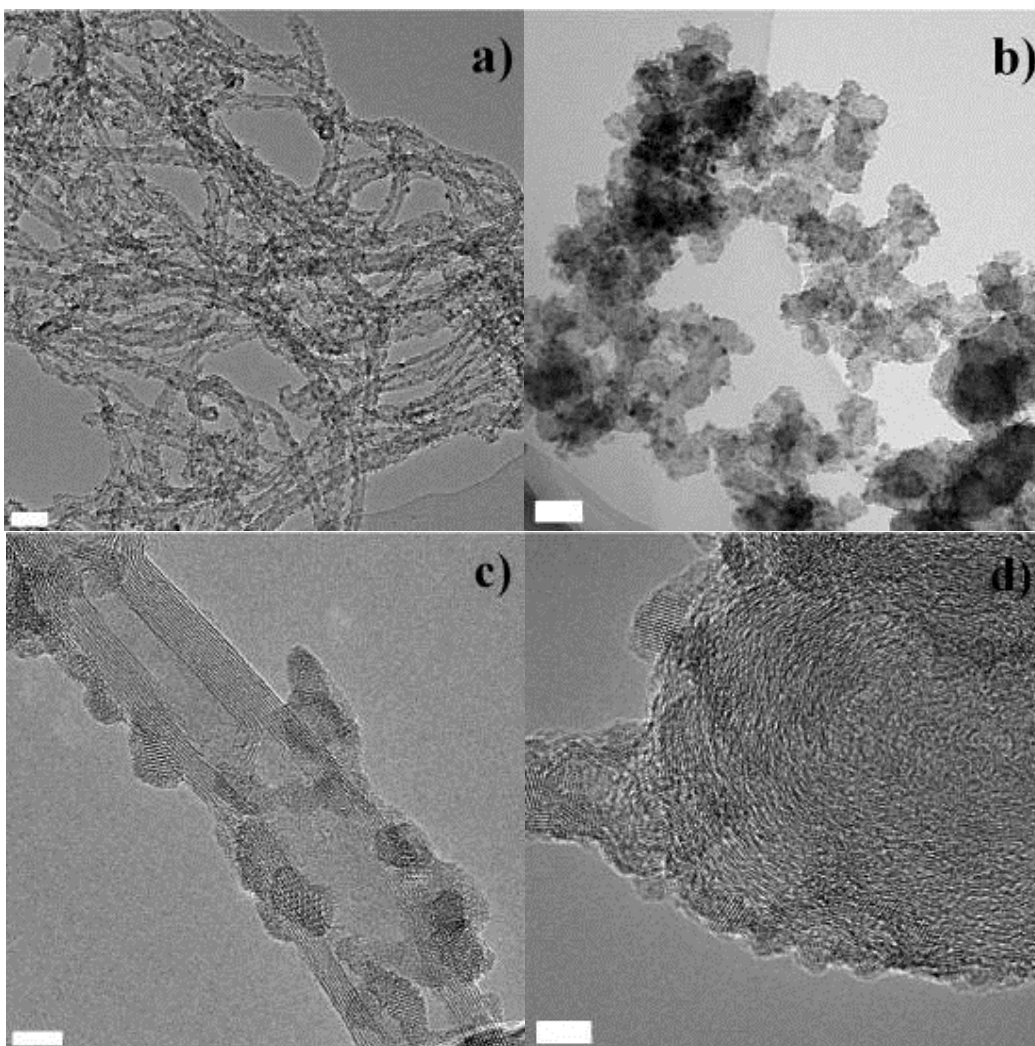


**Figure S4.** a) TEM image of anatase TiO<sub>2</sub>/CNTs, bar 50 nm. b) TEM image of anatase TiO<sub>2</sub>/carbon spheres (XC-72), bar 50 nm. c) HRTEM image of anatase TiO<sub>2</sub>/CNTs, bar 5 nm. d) HRTEM image of anatase TiO<sub>2</sub>/carbon spheres (XC-72), bar 5 nm.

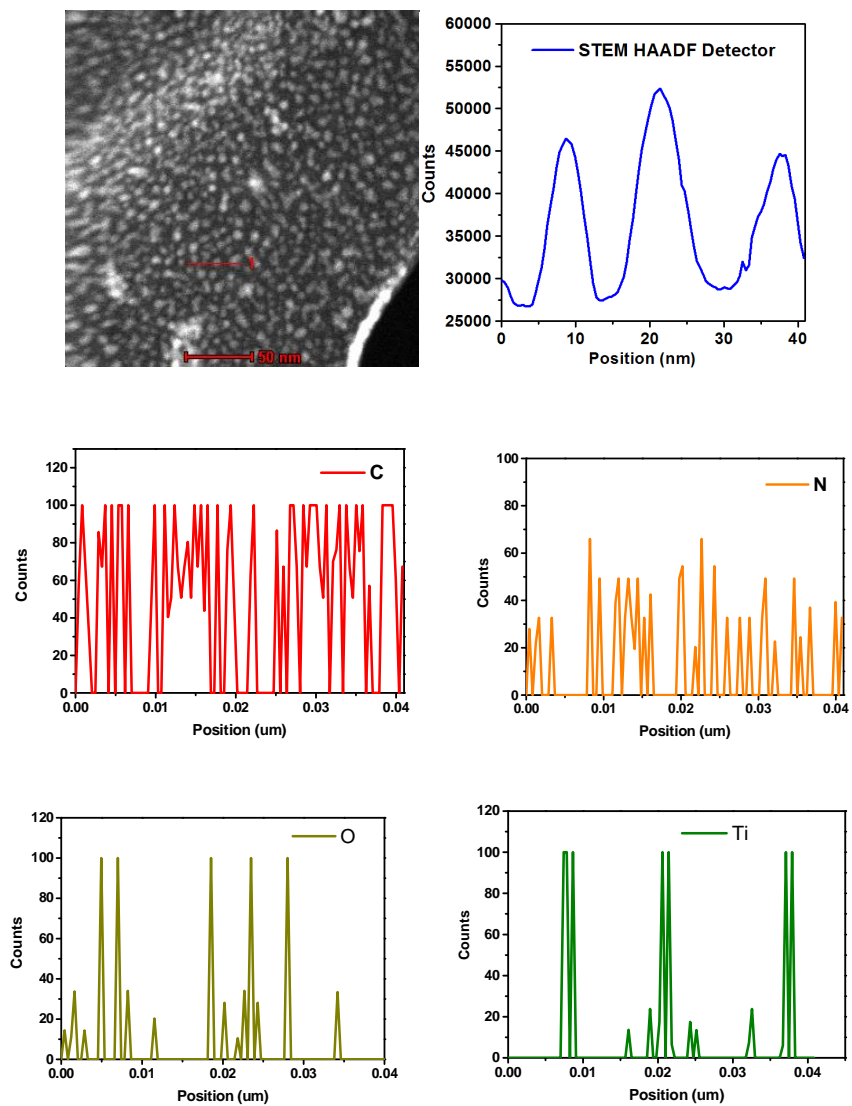


**Figure S5.** Energy-dispersive X-ray spectroscopy (EDS) line scan analysis based on the STEM-HAADF model demonstrating the distribution of C, N, O, and Ti species; while the Ti and O species are dispersed on the particles, the C and N species are dispersed along the line.

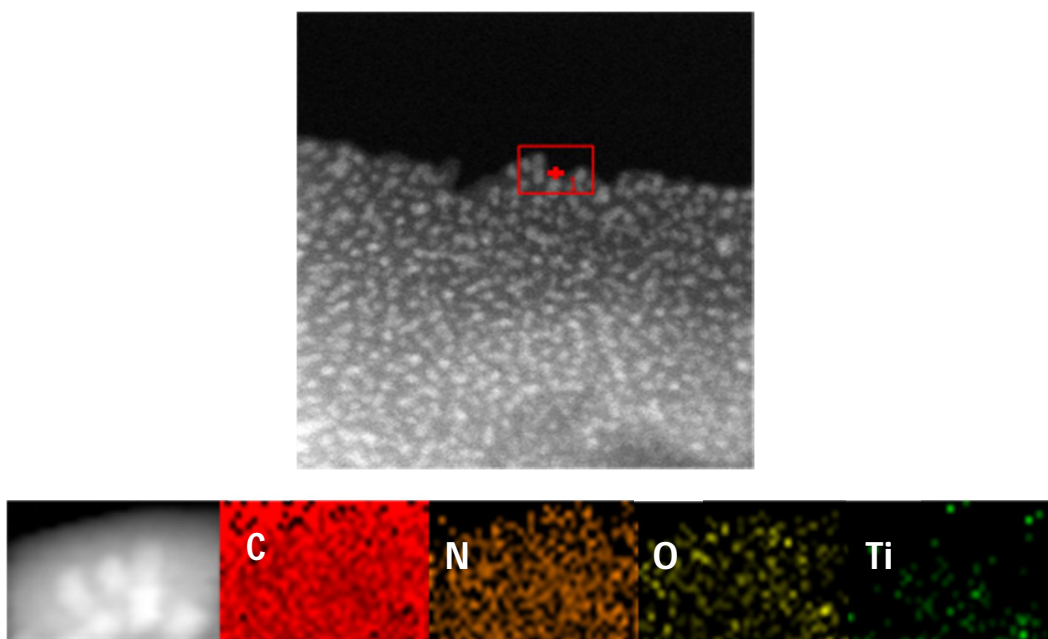


**Figure S6.** EDS elemental mapping of C, N, O, and Ti species for the anatase TiO<sub>2</sub>/RGO composite.

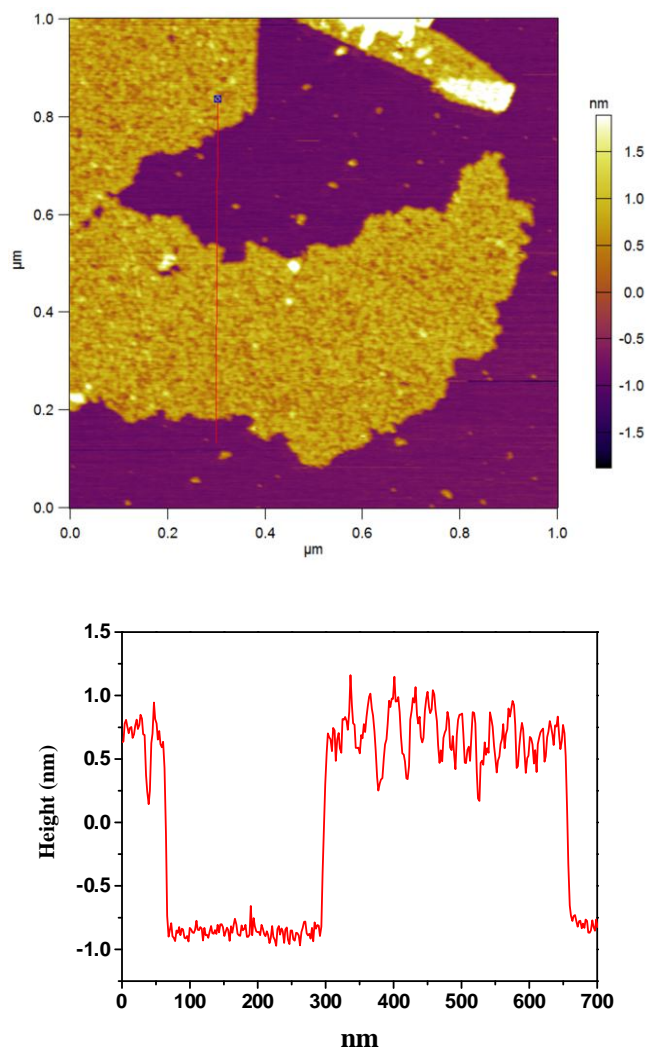


**Figure S7.** Topography image of GO on a mica substrate and the corresponding height-profile analysis along the line.

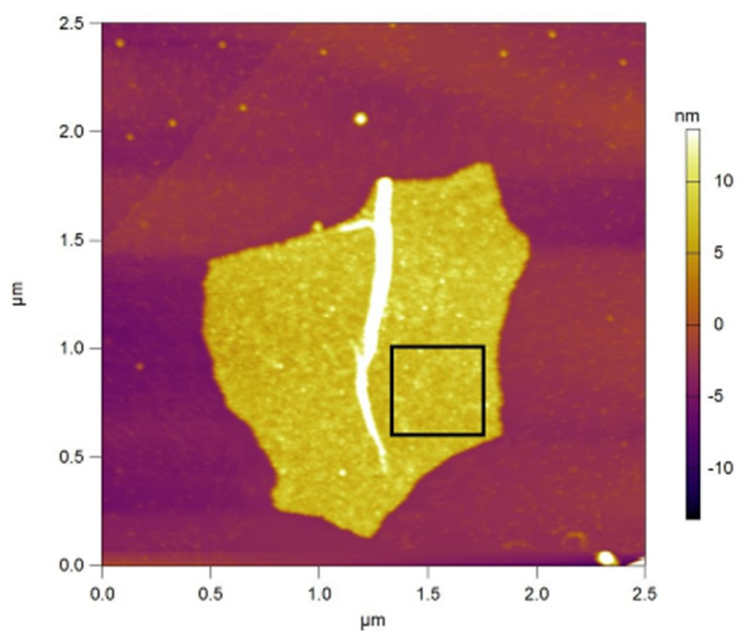


**Figure S8.** Topography image of anatase TiO<sub>2</sub>/RGO on the HOPG substrate; the black square region is ready for current image collecting.

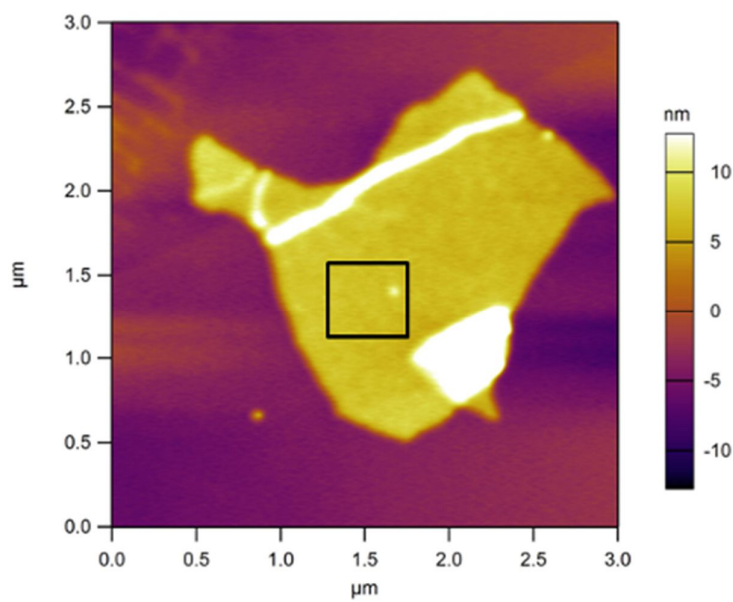


**Figure S9.** Topography image of amorphous TiO<sub>2</sub>/GO on the HOPG substrate; the black square region is ready for current image collecting.



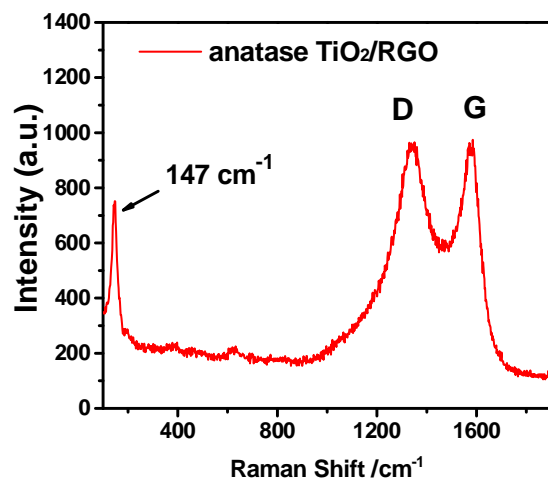


**Figure S10.** Raman spectrum of the anatase TiO<sub>2</sub>/RGO composite.

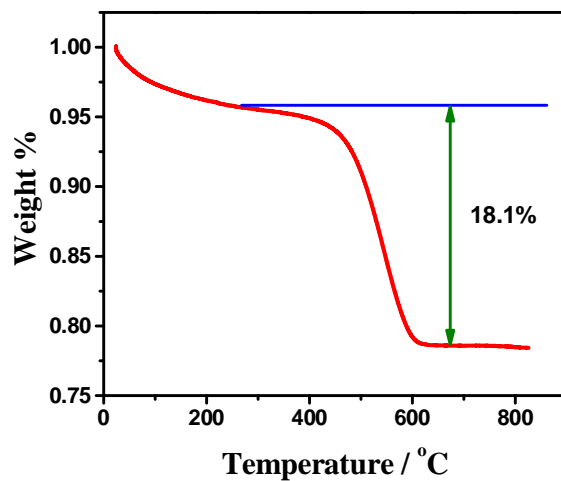


**Figure S11.** TGA analysis of the anatase TiO<sub>2</sub>/RGO composite in air.

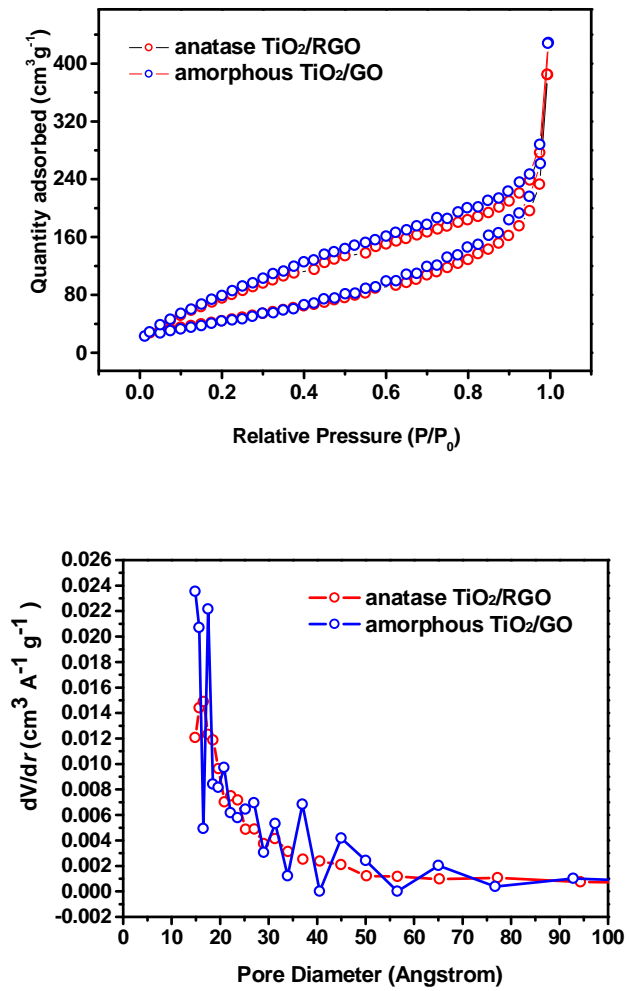


**Figure S12.**  $N_2$  adsorption/desorption isotherms of amorphous  $TiO_2/GO$  and anatase  $TiO_2/RGO$  composites and corresponding pore size distribution results analyzed by the BJH method.

**Table S1** Comparison of electrochemical performance of obtained anatase TiO<sub>2</sub>/RGO with other relative anodes materials.

Materials	Discharge density	Capacity (mAh g <sup>-1</sup> )	Cycle numbers	Reference
Anatase TiO <sub>2</sub> /RGO	5C	151	50	Current study
Anatase TiO <sub>2</sub> -FGS	1C	160	100	[9]
TiO <sub>2</sub> -RGO	5C	175	30	[11]
TiO <sub>2</sub> -RGO	5.9C	143	35	[16]
TiO <sub>2</sub> /GAs	5.9C	130	40	[18]
Graphene-TiO <sub>2</sub>	5C	130	100	[10]
TiO <sub>2</sub> -RGO	5C	152	100	[71]
TiO <sub>2</sub> –GNS –CNT	10C	111	100	[72]
Graphene-TiO <sub>2</sub> -C	0.59C	95	20	[73]